D1–D2–Cytochrome *b*559 Complex from the Aquatic Plant *Spirodela oligorrhiza*: Correlation between Complex Integrity, Spectroscopic Properties, Photochemical Activity, and Pigment Composition†

P. Braun,‡,§ B. M. Greenberg,‖,⊥ and A. Scherz*,‡,#

Biochemistry Department and Department of Plant Genetics, Weizmann Institute, Rehovot 76100, Israel

Received September 8, 1989; Revised Manuscript Received April 27, 1990

ABSTRACT: A D1–D2–cyt *b*559 complex with about four attached chlorophylls and two pheophytins has been isolated from photosystem II of the aquatic plant *Spirodela oligorrhiza* and used for studying the detergent-induced changes in spectroscopic properties and photochemical activity. Spectral analyses (absorption, CD, and fluorescence) of D1–D2–cyt *b*559 preparations that were incubated with different concentrations of the detergent Triton X-100 indicate two forms of the D1–D2–cyt *b*559 complexes. One of them is photochemically active and has an absorption maximum at 676 nm, weak fluorescence at 685 nm, and a strong CD signal. The other is photochemically inactive, with an absorption maximum at 670 nm, strong fluorescence at 679 nm, and much weaker CD. The relative concentrations of the two forms determine the overall spectra of the D1–D2–cyt *b*559 preparation and can be deduced from the wavelength of the lowest energy absorption band: preparations having maximum absorption at 674, 672, or 670.5 nm have approximately 20, 60, or 85% inactive complexes. The active form contains two chlorophylls with maximum absorption at 679 nm and CD signals at 679 (+) and 669 nm (−). These chlorophylls make a special pair that is identified as the primary electron donor P-680. The calculated separation between the centers of these two pigments (using an extended version of the exciton theory) is about 10 Å, the pigments' molecular planes are tilted by about 20°, and their N_1–N_3 axes are rotated by 150° relative to each other. The other two chlorophylls and one of the two pheophytins in the D1–D2–cyt *b*559 complex have their maximum absorption at 672 nm, while the maximum absorption of the photochemically active pheophytin is probably at 672–676 nm. During incubation with Triton X-100, the photochemically active complex is transformed into an inactive form with first-order kinetics. In the inactive form the maximum absorption of the 679 nm absorbing Chls is blue-shifted to 669 nm. The first-order decay of the photochemical activity suggests that the isolated D1–D2–cyt *b*559 complex is stable as an aggregate but becomes unstable on dissociation into individual D1–D2–cyt *b*559 units.

Light-induced electron transfer from a primary electron donor (P) to a primary electron acceptor (I) in the photosynthetic reaction center (RC) results in the formation of an electrochemical potential that drives biological photosynthesis (Okamura et al., 1982). Although the RCs of nonoxygenic bacteria have been characterized in great detail, there is still controversy about the electron-transfer mechanism in the early steps of photosynthesis. [For a recent review of possible mechanisms, see Warshel et al. (1988)]. Structural and functional characterization of the oxygenic RCs, followed by comparison to nonoxygenic ones, could reveal further information on the nature of the primary reactants and the underlying mechanisms of photosynthetic charge separation.

Among other important results, the recent X-ray crystallographic studies of bacterial RCs (Deisenhofer et al., 1985; Chang et al., 1986; Allen et al., 1987) have confirmed the pigments' organization roughly determined by other spectroscopic techniques. Of particular importance is the observation of a special pair of bacteriochlorophylls (Bchls), which had been predicted to constitute the primary electron donors P-860 and P-960 in *Rhodobacter* (*Rb.*) *sphaeroides* and *Rhodopseudomonas* (*Rps.*) *viridis*, respectively, by paramagnetic resonance (Norris et al., 1971, 1975; Feher et al., 1975), optical detection of magnetic resonance (Den Blanken et al., 1982), absorption (Vermeglio & Clayton, 1976), and circular dichroism (CD) (Shuvalov & Asadov, 1979; Parson et al., 1984; Scherz & Parson, 1984b). Hence, it might be possible to roughly determine the pigment organization in the oxygenic RCs by spectroscopic techniques.

Nanba and Satoh (1987) recently isolated from the oxygen-evolving photosystem II (PSII) a chlorophyll–protein complex that has features similar to those of the bacterial RC. First, the isolated complex, termed D1–D2–cyt *b*559, can sensitize light-induced electron transfer (Nanba & Satoh, 1987; Barber et al., 1987a,b; Chapman et al., 1988; McTavish, 1989; Wasielewski et al., 1989). Second, it contains two major polypeptides, termed D1 and D2, that have significant homologies to the L and M apoproteins of the bacterial RC (Williams et al., 1984; Hearst et al., 1984; Trebst & Depka, 1985; Michel & Deisenhofer, 1988). Third, the D1–D2 polypeptide complex binds four or five chlorophylls *a* (Chl*a*) to each two pheophytin *a* (Phe*a*) molecules, one non-heme iron and one β-carotene (Barber et al., 1987a; Nanba & Satoh, 1987; Van Dorssen et al., 1987; Satoh, 1989). In the PSII core complex, the D1 polypeptide binds plastoquinone molecules as well (Marder et al., 1986). This composition resembles that of the bacterial RC, where one finds four bacteriochlorophylls (Bchl), two bacteriopheophytin (Bphe), two

† This study was financially supported by the U.S.–Israel Binational Science Foundation (Grant 84-00144).

* Author to whom correspondence should be addressed.
‡ Biochemistry Department.
§ In partial fulfillment of a Ph.D. Thesis.
‖ Department of Plant Genetics.
⊥ NIH postdoctoral fellow in the Weizmann Institute of Science. Current address: Departmen of Biology, University of Waterloo, Waterloo, Ontario N2L-3G1, Canada.
Recanati Career Development Chair.

0006-2960/90/0429-10376$02.50/0

quinones, one non-heme iron, and one carotenoid. However, Dekker et al. (1989) have recently claimed that there are approximately 11 chlorophylls to each 2–3 pheophytins and 2 cyt *b*559 in the PSII RCs. This would imply that the D1–D2–cyt *b*559 complex contains a much larger number of Chls than previously thought and that RC is made of two D1–D2–cyt *b*559 complexes.

Further characterization of the PSII RC has been hampered by the variability of its spectroscopic properties. The position of the lowest energy absorption maximum of different D1–D2–cyt *b*559 preparations varies between 670 nm (Van Dorssen et al., 1987), 672 nm (Newell et al., 1988), 673–674 nm (Nanba & Satoh, 1987; Tetenkin et al., 1989), and 676 nm (Seibert et al., 1988; Scherz et al., 1988a,b; Breton, 1989). Different shapes for the CD signals have been reported by Van Dorssen et al. (1987) and by Newell et al. (1988). Different values also have been reported for the fluorescence intensity and band position (Van Dorssen et al., 1987; Newell et al., 1988). The spectroscopic variability was accompanied by inconsistency of the reported quantum yield of photochemical activity (Takahashi et al., 1987; Chapman et al., 1988; McTavish et al., 1989) and was suggested to reflect an instability of the isolated PSII RC (Braun et al., 1988; Scherz et al., 1988a,b; Seibert et al., 1988).

The origin of the spectral instability of the isolated D1–D2–cyt *b*559 complex and its relation to the photochemical activity are not clear. Seibert et al. (1988) and McTavish et al. (1989) could keep a D1–D2–cyt *b*559 complex with relatively high photochemical activity for hours by replacing the TX-100 [a detergent added to separate the PSII RC core complex (Satoh, 1989) into smaller components] with lauryl maltoside (LMa). However, the LMa–D1–D2–cyt *b*559 complex has maximum optical absorption at 674 nm, whereas three reports have indicated that the maximum absorption of a freshly isolated D1–D2–cyt *b*559 complex is at 676 nm (Scherz et al., 1988a,b; Seibert et al., 1988; Breton, 1989). Furthermore, although the rate of the absorption blue shift was profoundly slowed down, using LMa instead of the TX-100 could not prevent a shift to 673–674 nm in about 2 days even when the sample was stored at 4 °C and in the dark. This could mean that the detergent effect on the spectral properties and the photochemical activity of the isolated PSII RCs is not limited to TX-100.

The spectral difference between the LMa-stabilized D1–D2–cyt *b*559 preparation and the freshly isolated one could indicate either that the former is a heterogeneous sample that contains some disintegrated complexes (Braun & Scherz, 1988) or that it is a homogeneous solution of a slightly modified yet fully active form of the PSII RC (McTavish et al., 1989, Tetenkin et al., 1989). Since a meaningful characterization of the complex depends on whether the preparation is photochemically active or not, there is a need to correlate the integrity of the D1–D2–cyt *b*559 complex with its spectral properties. Such a correlation may provide guidelines for increasing the stability of the complex and at the same time shed light on the assembly of the D1–D2 polypeptides and their prosthetic groups. To that end, we have incubated different concentrations of the D1–D2–cyt *b*559 complex from *Spirodela oligorrhiza* in TX-100-containing buffer, while examining their spectra (absorption, CD, and fluorescence) and photochemical activity. Preliminary reports have been given by Braun and Scherz (1988) and by Scherz et al. (1988a,b).

Materials and Methods

Isolation of the D1–D2–Cyt b559 Complex. The D1–D2–cyt *b*559 complex was isolated from the aquatic plant *S. oligorrhiza* grown on half-strength Hutner's medium (Posner, 1967) following a modification of the procedure reported by Marder et al. (1987). Plant tissue was disrupted in an ice-cold medium consisting of 0.4 M sucrose, 10 mM Tricine, (pH 8.0), 10 mM NaCl, and 10 mM $MgCl_2$ with a blender fitted with razor blades and then homogenized in a motor-driven glass/glass tissue grinder. The crude homogenate was passed through one layer of Miracloth (Calbiochem) and the filtrate centrifuged for 1 min at 500*g* to pellet unbroken cells and other large fragments. The supernatant was subjected to further centrifugation at 3000*g* for 12 min to obtain the thylakoid fraction. The membrane fraction was washed with 20 mM Tricine (pH 8.0) containing 150 mM NaCl and 10 mM $MgCl_2$ and recentrifuged, and the resulting pellet was suspended in 20 mM MES/10 mM $MgCl_2$ (pH 6.5) to a Chl*a* concentration of ≈2 mg/mL. After the addition of TX-100 [Chl:TX-100 = 1:21 (w/w)], the suspension was incubated for 20 min in the dark at 4 °C. Solubilized membranes were separated from the incubated suspension by centrifugation at 18000*g* for 40 min and then treated with 4% TX-100 (v/v) in 50 mM Tris (pH 7.2) for 1 h on ice in the dark with stirring. This was followed by centrifugation of this mixture for 1 h at 100000*g*. The resulting supernatant was layered onto a DEAE-Fractogel (Merck) ion exchange column that was equilibrated with 50 mM Tris buffer (pH 7.2) containing 0.2% Triton X-100. The majority of the chlorophyll added to the column was removed by extensive washing with the 0.2% Tris/TX-100 buffer containing 30 mM NaCl. Purified D1–D2–cyt *b*559 complex was eluted by a continuous NaCl gradient (30–400 mM) in the Tris/TX-100 buffer. All preparation steps were performed at 4 °C. The D1–D2–cyt *b*559 fraction was identified by optical spectroscopy and sodium dodecyl sulfate–polyacrylamide gel electrophoresis (Figure 1).

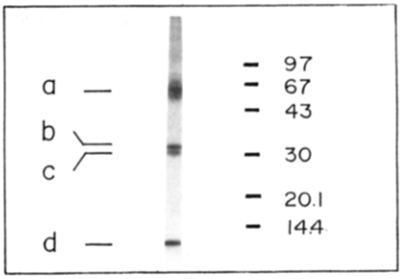

FIGURE 1: Polyacrylamide gel electrophoreses of the D1–D2–cyt *b*559 complex from *S. oligorrhiza*. Electrophoresis was carried out on SDS slab gels containing a 10–20% gradient of polyacrylamide with a 5% stacking gel (Laemmli, 1970). The major D1–D2–cyt *b*559 fractions from the DEAE-Fractogel column (30 μL) were loaded along with sample buffer (8 μL of 3% SDS). After running, the gel was stained with Coomasie Blue. The positions of prestained molecular size markers (from Pharmacia; given in kDa) in sample buffer are indicated by tick marks. (a) D1–D2 aggregates; (b) D21; (c) D2; (d) cyt *b*559 (α subunit).

Analyses of the Porphyrin Content of the D1–D2–Cyt b559 Complex. The Chl*a* and Phe*a* content of the D1–D2–cyt *b*559 complex was determined as follows. The chromophores were extracted into 3:1 ethanol:hexane. The hexane phase was separated and dried. The Chl*a*/Phe*a* mixture was redissolved in acetone for high-pressure liquid chromatography in 1:9 (v/v) acetonitrile:methanol with a C18, reversed-phase, 25.00 × 0.46 cm Vydac TP20154 column [after Ben-Amotz et al. (1989)] or for immediate spectroscopic analysis. To determine the Chl*a* and Phe*a* content from the mixtures' spectrum in acetone, we employed

$$x = 0.013(OD_{411} - 0.54OD_{482}) - 0.012OD_{662}$$
$$y = 0.018OD_{662} - 0.009(OD_{411} - 0.54OD_{482}) \quad (1)$$

where x and y give the millimolal concentrations of Phe*a* and Chl*a*, respectively, using the specific extinction coefficients of Chl*a* and Phe*a* at 411 and 662 nm in wet acetone (Lichtenthaler, 1987). OD_{411}, OD_{482}, and OD_{662} are the experimental optical densities at 411, 482, and 662 nm, respectively. The cyt *b*559 level was determined as described by Barber et al. (1987b).

Determination of the Pigment to Protein Ratio. The protein content of the D1–D2–cyt *b*559 preparation was determined by the Bradford reaction with Bio-Rad (Bio-Rad Laboratories) reagents. For protein standards we used bovine serum albumin, purified PSII light-harvesting complexes (LHII), and RCs from the purple bacterium *Rb. sphaeroides*. The pigment content in the green plant complexes was determined from their absorption at ~676 nm by each of the following methods: (a) by use of an extinction coefficient of 74 mM^{-1} cm^{-1} as recommended by Dekker et al. (1989); (b) by use of formula 1 as described earlier; (c) from the Phe*a* content after pheophytinization of the Chls (Vernon, 1960) with extinction coefficients of $\epsilon_{665} = 51.88$ and $\epsilon_{408} = 126$ mM^{-1} cm^{-1}. The bacteriochlorophyll content in the bacterial RCs was determined from their absorption at 855 nm with an extinction coefficient of 1.3×10^5 M^{-1} cm^{-1} (Straley et al., 1973). The protein content in the bacterial RCs and LHII determined with the albumin standard had to be divided by 2 to match the value determined from the spectroscopic measurements.

Depletion of TX-100. TX-100 was removed from the D1–D2–cyt *b*559 preparation by addition of up to 1 g of SM-2 Bio-Beads (Bio-Rad) for each 34 μg of Chl*a* and incubation on ice for 2 h in the dark. The depletion of the TX-100 was followed by measurement of the absorption at 275 nm (where TX-100 in Tris buffer has a relatively narrow absorption band). Partial removal of TX-100 was achieved by incubation with reduced amounts of SM-2 Bio-Beads. The residual concentration of the detergent was determined from the absorption at 275 nm with

$$[\text{TX-100}] = (OD_{275}^{exp} - OD_{275}^{D1D2})/\epsilon_{275}^{TX-100} \quad (2)$$

where $\epsilon_{275}^{TX-100} = 22$ is the absorbance of Tris [0.02 M, pH 7.2, 30–400 mM NaCl/TX-100 (1%)] in a 1-cm cuvette at 275 nm, OD_{275}^{exp} is the experimental optical density (OD), and OD_{275}^{D1D2} is optical density of the TX-100-depleted complex including scattering effects.

Measurement of Photochemical Activity. The photochemical activity of the D1–D2–cyt *b*559 complex was determined by following the reversible absorbance changes due to photochemical accumulation of Phe*a* under the reducing conditions described by Nanba and Satoh (1987). An Aminco dual-wavelength spectrophotometer (in the split-beam mode) equipped with a 300-W quartz–iodine actinic lamp (supplied with a heat filter and an additional Schott RG-665 filter) was used to read the absorbance change after 30 s of illumination. The samples' temperature was kept at 3–4 °C, and the light intensity at the cuvette surface was 2400 μE m^{-2} s^{-1}. A solution of $CuSO_4$ was positioned in front of the photomultiplier. The photochemical activity was measured for complexes that had been incubated (on ice in the dark) either with 0.2% TX-100 or with no TX-100. To solubilize aggregates formed in the TX-100-depleted preparation, the sample was mixed with Tris buffer containing 0.2% TX-100, to a final concentration of 0.1%, just before the measurement of photochemical activity.

Measurement of Optical Absorption, CD, and Fluorescence. Optical absorption spectra were recorded by a computerized Milton-Roy Spectronics 1201 spectrophotometer. CD spectra were obtained on a home-built, computerized dichrograph. Fluorescence was measured by a Perkin-Elmer MPF44 fluorometer. All measurements were made at 4 °C.

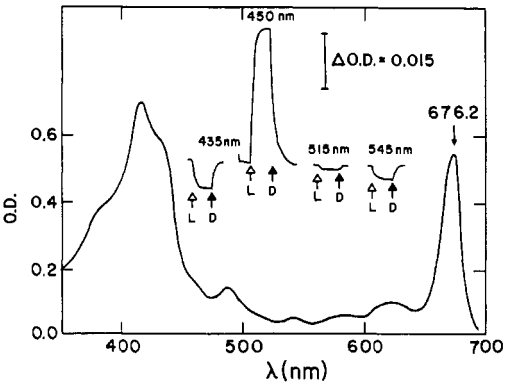

FIGURE 2: Optical absorption of a D1–D2–cyt *b*559 complex from *S. oligorrhiza* in Tris (0.05 M, pH 7.2)/TX-100 (0.2%), immediately after separation from a DEAE–Fractogel column. (Insert) Reversible absorption changes after addition of 1 μM methyl viologen and 1 mg of sodium dithionite per 1 mL of the complex and illumination for 30 s. The conditions for illumination are given under Materials and Methods.

Spectra Deconvolution and Derivation. Spectra deconvolution into Gaussians was carried out by an IBM mainframe computer using the programs CURFIT (written in Fortran) and CDMASTER (written in Turbo Pascal). The accuracy of this method and its applicability to Chl aggregates are discussed elsewhere (Katz et al., 1978; Uehara et al., 1988). The programs first convert the experimental spectra from wavelength (λ) to wavenumber (cm^{-1}) domain. Then, they search for second and fourth derivatives, from which the peaks' locations are deduced. The contribution of higher energy bands (e.g., the Q_4y^{0-1} transitions of the Chls and the Phes) to the lowest energy band (i.e., the Q_y^{0-0} transition) is found and subtracted from the experimental curve, and the difference is fitted with the minimum number of Gaussians or Lorentzians. The goodness of fitting is given by $\eta = (1/n)\sum_{i=1}^{n}(z - x)_i^2/x_i^2$, where z and x are the calculated sum of the resolved Gaussians and the experimental reading at i nm, respectively, and n is the number of readings. The calculated spectrum is converted back to the wavelength domain for presentation.

RESULTS

Pigment Content of the D1–D2–Cyt b559 Complex. The porphyrin to protein ratio in the D1–D2–cyt *b*559 complexes isolated as described was determined to an average value of five to seven porphyrins per 78-kDa protein complex. The number of Chl*a* molecules to each Phe*a* determined by HPLC ranges from 2.15 to 2.5. The ratio obtained from analyses of the acetone extract is ≈2.20. For each four Chl*a* we found one cyt *b*559. Combining these data with the ratio of five to seven porphyrins to each 78-kDa protein, we conclude that the D1–D2–cyt *b*559 complex that has been isolated from *S. oligorrhiza* as described contains four Chl*a*, two Phe*a*, and one cyt *b*559 molecule. The slight deviation that is observed experimentally could be due to (a) minor contamination (<-0.2%) with CP47, (b) free Chls that absorbed to the TX-100–D1–D2 complex in the early steps of the ion exchange chromatography, and (c) inaccuracy of the HPLC method.

Spectroscopic Properties and Photochemical Activity of the Freshly Isolated D1–D2–Cyt b559 Complex. The optical absorption spectrum of the isolated D1–D2–cyt *b*559 PSII RC measured immediately after separation from the ion exchange column is shown in Figure 2. A similar absorption spectrum was reported for an 85-kDa D1–D2–cyt *b*559 complex (Thornber et al., 1988) isolated from thylakoid membranes by "green gel" electrophoresis (Thornber et al., 1986, 1987;

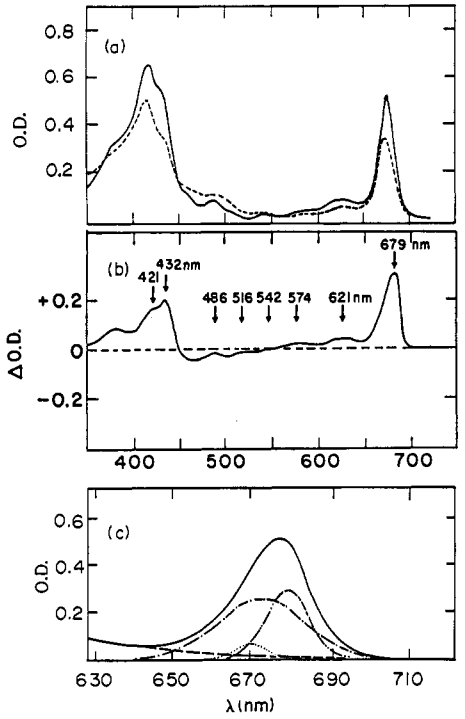

FIGURE 3: (a) Optical absorption spectra of freshly prepared D1–D2–cyt *b*559 complex (—) and a D1–D2–cyt *b*559 complex that have been continuously illuminated for 20 min at 4 °C by white light (200 $\mu E/m^2$) (– –). Spectra were recorded at 4 °C. (b) Difference spectra between nonilluminated and illuminated D1–D2–cyt *b*559 complex. (c) Gaussian convolution of the D1–D2–cyt *b*559 lowest energy absorption: (–··–) 679-nm component; (–·–) 672-nm component; (···) 669-nm component; (– –) tail of higher energy transitions (Q_y^{0-1}); (—) sum of the Gaussian components.

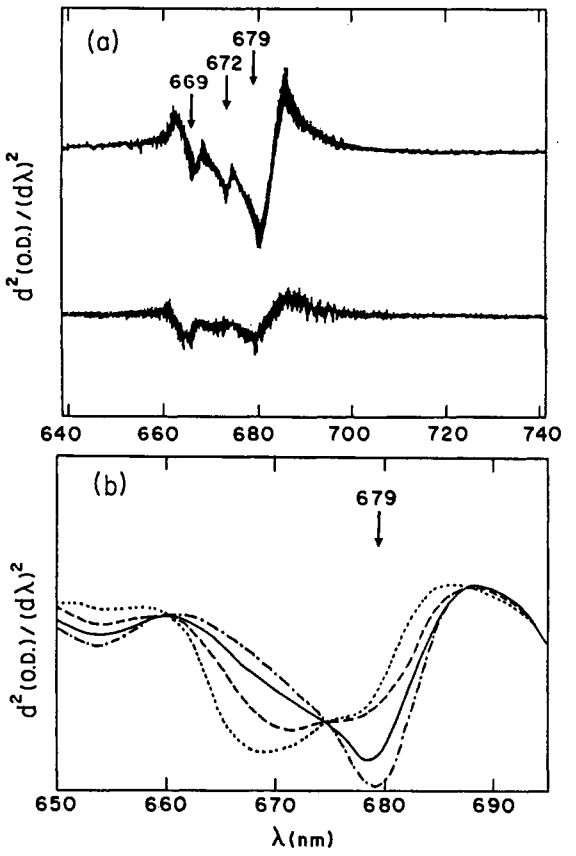

FIGURE 4: (a) Second derivative of a D1–D2–cyt *b*559 optical absorption. (Upper trace) Absorption derivative of a freshly isolated complex. (Lower trace) Absorption derivative of a complex after 3 days of incubation on ice in the dark. (b) Second absorption derivatives of D1–D2–cyt *b*559 complexes during incubation in Tris (0.02 M, pH 7.2)/TX-100 (0.2%) on ice in the dark and after smoothing: (–·–) freshly isolated complex (maximum OD at 676 nm); (—) 2 h of incubation (maximum OD at 674 nm); (– –) 24 h of incubation (maximum OD at 672 nm); (···) 100 h of incubation (maximum OD at 671 nm).

Peter et al., 1988, 1989). The 676 nm absorbing D1–D2–cyt *b*559 isolated in the present study also migrates as an 85-kDa complex, on polyacrylamide gels with the nondenaturing system of Thornber et al. (1988) (Braun and Scherz, unpublished data).

As previously reported (Scherz et al., 1988a,b; Seibert et al., 1988), the freshly isolated D1–D2–cyt *b*559 complexes had absorption maxima at 676–677, 543, 483, and 416 nm. Reversible bleaching at 430, 515, and 545 nm as well as a reversible absorption increase at 450 nm could be induced by illumination (Figure 2 insert) for a period of 30 s in the presence of sodium dithionite (1 mg/mL) and methyl viologen (1 μM). Continuous illumination with low light intensity (200 $\mu E\ m^{-2}\ s^{-1}$) in the absence of dithionite and methyl viologen irreversibly bleached ≈35% of the lowest energy absorption band and ≈25% of the absorption at 432 nm. The spectra of illuminated and nonilluminated samples and their difference are shown in Figure 3a,b. The difference spectrum is nearly identical with that of P-680 (Van Gorkom et al., 1975), with peaks at 679, 621, 486, and 432 nm.

The second derivative of the absorption spectrum of freshly isolated D1–D2–cyt *b*559 complexes reveals that the 676 nm absorption band consists of two major components with maxima at 679 and 672 nm and a minor component with a maximum at 669 nm (Figure 4a).

The CD spectrum of the 676 nm absorbing D1–D2–cyt *b*559 complex (Figure 5a) is markedly different from the CD spectra of Chl*a* and Phe*a* monomers in vitro (Houssier & Sauer, 1970) but resembles the spectrum of Chl*a* dimers and larger aggregates in vitro (Houssier & Sauer, 1970; Figure 5b). In the lowest energy region, the CD signal peaks at 682 nm (+) and 666 nm (–) and contains two components. Only one of these two components bleaches upon continuous illumination in the absence of reducing agents (Figure 5c). The light-dependence CD can be fitted by two Gaussians (using the CURFIT program) with maximum intensity at 679 nm (+) and 669 nm (–). The light-independent CD signal can be fitted by two Gaussians that peak at 673 nm (+) and 671 (–) (Figure 5e).

The fluorescence of freshly prepared D1–D2–cyt *b*559 complexes is shown in Figure 6a. It peaks at 685 nm and has very low intensity.

Detergent-Induced Spectral Changes of the D1–D2–Cyt b559 Complex. Incubation in Tris (0.05 M, pH 7.2)/TX-100 (0.2%) solution on ice in the dark shifted the long-wavelength absorption band of the freshly isolated D1–D2–cyt *b*559 complex to a shorter wavelength (Figure 7a). At the same time, the intensity of the second absorption derivative decreased at 679 nm and increased at 669 nm, with the different curves having several isosbestic points (Figure 4b). The second derivative spectrum after 24 h of incubation (lower curve in Figure 4a) is similar to the one published by Satoh (1989) and by Losche et al. (1989). The change in the optical absorption is accompanied by a decrease of the CD signal, which eventually flattens out (Figure 5c). A blue shift of the fluorescence maximum from 685 nm (Figure 6a) to 679 nm (Figure 6b) is observed, accompanied by a 20-fold increase in the fluorescence intensity.

The differences between the absorption spectrum of the freshly isolated D1–D2–cyt *b*559 complex and the spectra taken at different incubation times are plotted in Figure 7b.

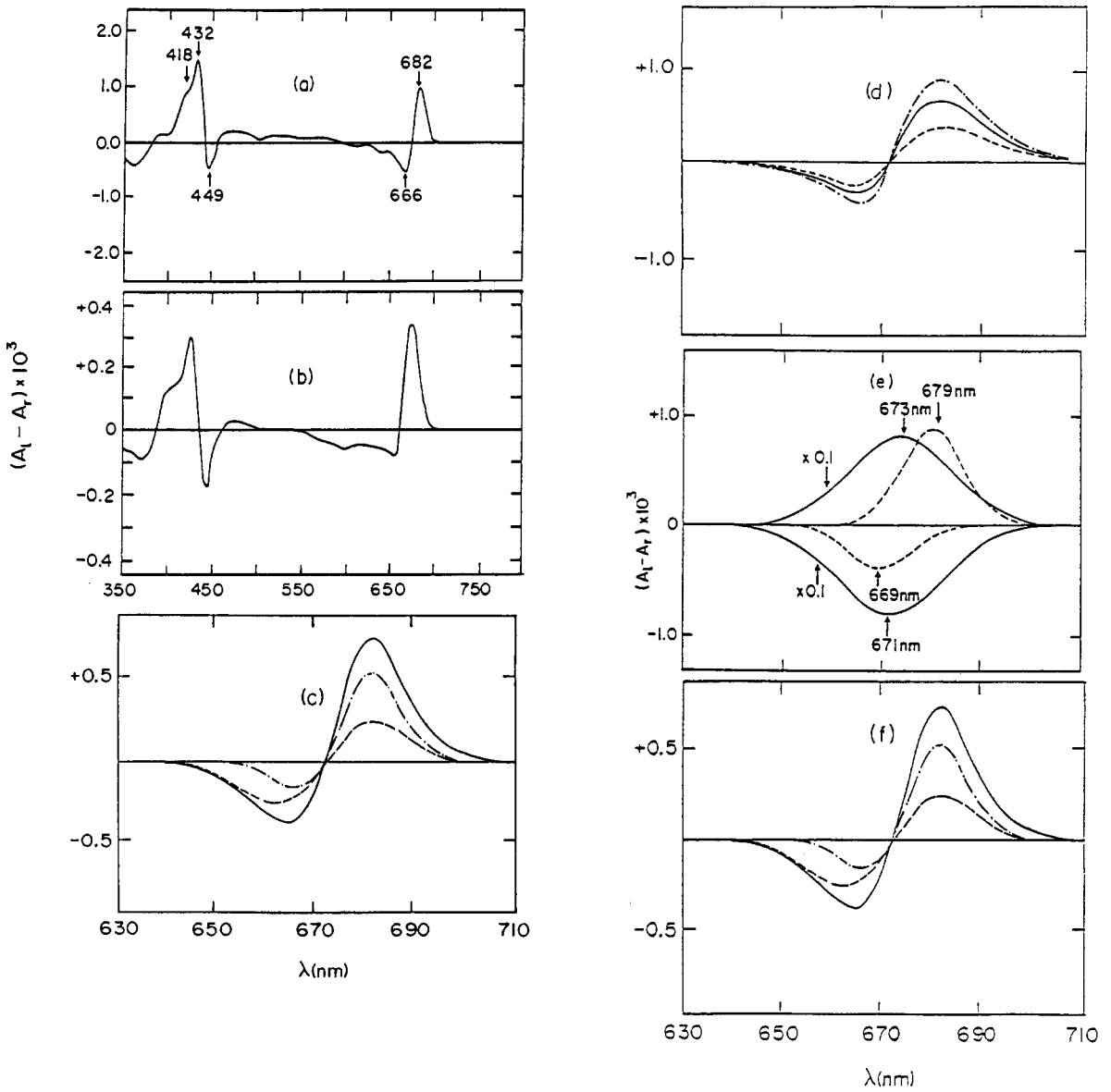

FIGURE 5: (a) CD spectrum of a freshly prepared D1–D2–cyt *b*559 complex recorded at 4 °C. (b) CD spectrum of Chl*a* dimers in CCl_4 [taken from Houssier and Sauer (1970)]. (c) Lowest energy CD signal of a D1–D2–cyt *b*559 complex in Tris buffer solution containing 0.2% TX-100 (at 4 °C): (—) before illumination; (-·-) after illumination for 20 min with white light; (--) difference between the CD signal before and after illumination. (d) Lowest energy CD signal of a D1–D2–cyt *b*559 complex incubated in Tris buffer solution containing 0.2% TX-100 for (-·-) 10 min, (—) 2 h, and (--) 24 h. (e) Gaussian convolution of the lowest energy CD signal: (solid lines) components with 300 cm s^{-1} half-bandwidth; (dashed lines) components with 570 cm s^{-1} bandwidth. (f) (-·-) Sum of the 679- and 669-nm Gaussian couplets; (--) sum of the 673- and 671-nm Gaussian couplets; (—) sum of all four Gausians. (g) Lowest energy CD signal of (—) freshly prepared D1–D2–cyt *b*559 complexes; (--) complexes that have been illuminated by white light (200 μE m^{-2} s^{-1} m^2) for 20 min; (-·-) Difference between CD signals of the nonilluminated and illuminated complexes.

All difference spectra intersect at 672 nm and have maximum and minimum at the same wavelengths. Each of the difference spectra can be deconvoluted into the same two Gaussians: a narrow positive one with maximum intensity at 679 nm that decreases during incubation and a broad negative one with maximum intensity at 669 nm that is increased during the incubation. The conversion of the initial 679-nm Gaussian into the 669-nm Gaussian was accomplished in about 200 h. At that time the D1–D2–cyt *b*559 absorption at 630–700 nm could be fitted by the 669-nm Gaussian, a tail from the Q_y^{0-1} transitions and a 672-nm Gaussian. The same tail and 672-nm Gaussian fit the spectrum of the nonincubated complex when added to the initial 679-nm Gaussian (Figure 3c). The spectra of all the incubated complexes also could be fitted with the 679-, 672-, and 669-nm Gaussians plus the Q_y^{0-1} tail. Just after separation from the ion exchange column, the 679- and the 672-nm Gaussians contribute ≈25% and ≈65% of the oscillator strength, respectively, and the 669-nm Gaussian contributes less than 10%. The band widths of the 679- and the 672-nm Gaussians are 300 and 542 cm^{-1} at half-maximum intensity, respectively.

The decay kinetics of the 679-nm Gaussian component fits a single exponential (Figure 8a).

Removal of the TX-100 from the isolated D1–D2–cyt *b*559 complex by SM-2 Bio-Beads right after the complex had been eluted from the ion exchange column prevented the modification of the spectra. Figure 8b illustrates that in the TX-100-depleted preparation there is practically no decrease in the 679-nm absorption for a period of more than 6 days. The time dependence of the 679-nm absorption was examined with different initial concentrations of the D1–D2–cyt *b*559 complexes at a fixed TX-100 concentration and with different concentrations of TX-100 at a fixed D1–D2–cyt *b*559 concentration. In each case, the 679-nm component decayed with

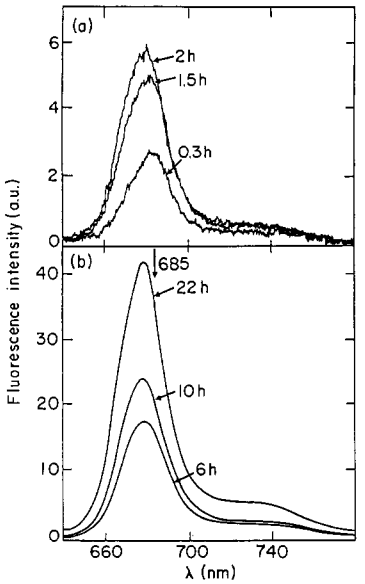

FIGURE 6: Changes in the fluorescence of the D1–D2–cyt *b*559 complex recorded at consecutive time intervals during incubation with 0.2% TX-100 at 0 °C. Initially, the complex has maximum OD at 676.2 nm, and spectra were recorded at 3–4 °C. (a) Within the first 2 h; (b) over the next 18 h.

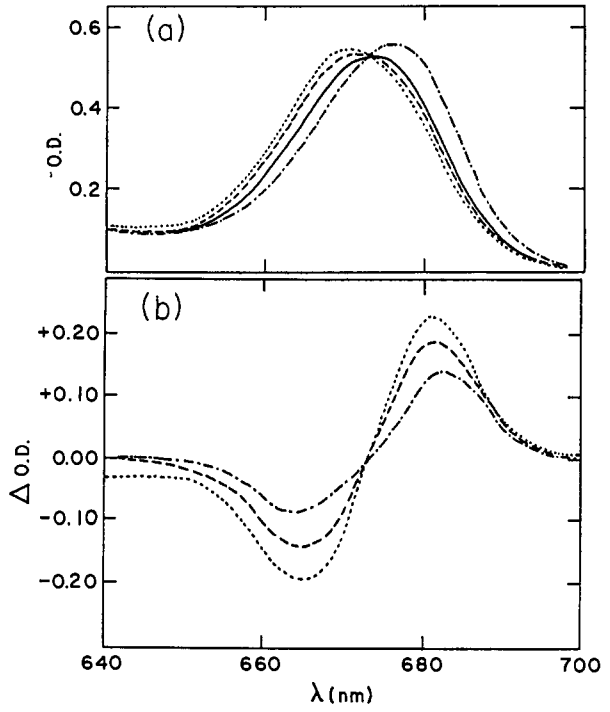

FIGURE 7: (a) Lowest energy absorption of a D1–D2–cyt *b*559 complex in a 1-cm cuvette recorded at consecutive times upon incubation in Tris (0.02 M, pH 7.2)/TX-100 (0.2%) on ice in the dark: (–·–) after 10 min; (—) after 24 h; (– –) after 100 h; (···) after 130 h. (b) Difference spectra between the optical absorption of a D1–D2–cyt *b*559 complex after separation from the ion exchange column (maximum OD at 676 nm in 1-cm cuvette equals 0.880) and spectra recorded at consecutive times of incubation in Tris (0.02 M, pH 7.2)/TX-100 (0.2%) on ice and in the dark: (–·–) after 24-h incubation; (– –) after 100-h incubation; (···) after 130-h of incubation.

a first-order kinetics. The value of the decay rate constant is inversely proportional to the initial OD of the 679-nm component (Figure 8a and 9) and roughly proportional to the concentration of TX-100 (not shown).

The maximum absorption of samples with TX-100 completely removed remained at 676–677 nm for more than 9 days, but the solution became highly turbid, reflecting an

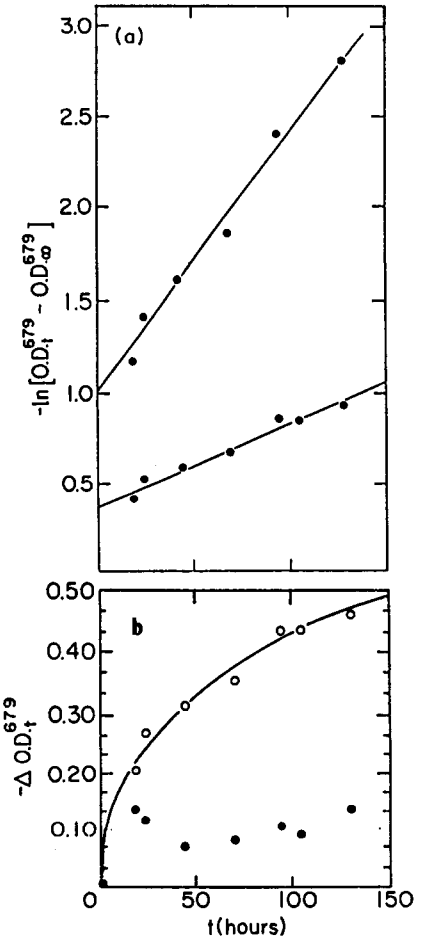

FIGURE 8: (a) Dependence of the 679-nm component on time during the incubation of the D1–D2–cyt *b*559 complex in Tris (0.02 M, pH 7.2)/TX-100 (0.2%). The initial absorption at 676-nm was 0.636 for the upper curve and 1.14 for the lower curve (in a 1-cm cuvette). OD_t^{679} is the OD of the D1–D2–cyt *b*559 complex after *t* h of incubation at 4 °C in a 1-cm cuvette; QD_∞^{679} is the OD of this complex after 210 h of incubation. (b) Time-dependent change of the 679-nm absorption of D1–D2–cyt *b*559 complexes incubated on ice in (○) Tris (0.02, pH 7.2)/TX-100 (0.2%) and in (●) Tris (0.02, pH 7.2)/TXH100 (0.0%). The initial OD of both samples was 0.880 at 676 nm. Note that in the absence of TX-100 there is a little bleaching of the 679 nm absorption band, right after separation (while incubated with the Bio-Beads), but no further bleaching could be observed.

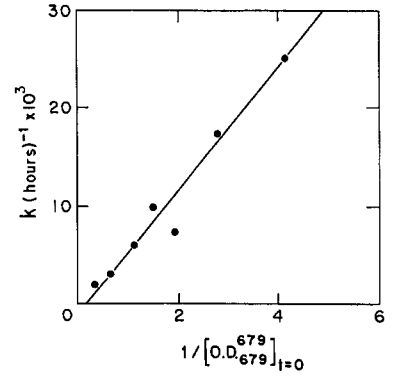

FIGURE 9: Dependence of the 679-nm decay constant *k* upon the initial OD of the 679-nm component. The D1–D2–cyt *b*559 complexes were incubated in Tris (0.02 M, pH 7.2)/TX-100 (0.2%). $k - d\ln(OD_t^{679} - OD_\infty^{679})/dt$.

aggregation of the D1–D2–cyt *b*559 complexes into large oligomers. The formation of such aggregates also was observed by McTavish et al. (1989).

Detergent-Induced Changes in the Photochemical Activity. The intensity of the light-induced reversible absorption change

Table I: Change in D1–D2–Cyt *b*559 Photochemical Activity and 679-nm Absorption during Incubation with Triton X-100

t^a	$\lambda_{max}{}^b$	$\Delta OD_t^{450}/\Delta OD_0^{450}{}^c$	[D1D2-679]^d
0	676	1.00	100
2	674	0.75	80
24	672	0.40	40
150	670.5	0.05	15

[a] Incubation time (in hours) of a D1–D2–cyt *b*559 preparation in TX-100. [b] Wavelength of the long-wavelength absorption band. [c] Reversible light-induced absorbance change at 450 nm after *t* h of incubation in 0.2% TX-100 relative to the initial light-induced absorbance change. [d] Percentage of active D1–D2–cyt *b*559 complex resolved by eq 3.

at 450-nm (Figure 2 inset) was continuously decreased during incubation. This decrease paralled the blue shift of the long-wavelength absorption bands, as shown in Table I. The aggregates formed in TX-100-depleted samples show no significant absorption change at 450 nm upon illumination. However, the addition of TX-100 to a final concentration of 0.1% (in Tris buffer) restored the ability of the D1–D2–cyt *b*559 complex to photoaccumulate reduced Phe*a* as reflected in the reversible absorption at 450 nm during illumination (≥75% of the initial value).

Discussion

Phenomenological Classification of the D1–D2–Cyt b559 Chromophores. Gel electrophoresis of the D1–D2–cyt *b*559 complex under nondenaturing conditions shows that the 676 nm absorbing D1–D2–cyt *b*559 complex migrates as an 80–85-kDa protein (Thornber et al., 1986, 1987; Peter & Thornber, 1988, 1989). The pigment to protein ratio and pigment stoichiometry found in the present study show that this 80–85-kDa complex holds about six porphyrins (four Chl*a* and two Phe*a* molecules). When the D1–D2–cyt *b*559 complex is separated from the ion exchange column, by use of a TX-100-containing eluting solution, the 676–677-nm absorption (Figure 2) consists of two major Gaussian components. One component peaks at 679 nm and the other at 672 nm (Figure 3c). There is also a minor Gaussian component that peaks at 669 nm. Upon incubation with TX-100, the 679-nm component decays, and the 669-nm Gaussian grows at the same rate. No change is observed in the 672-nm component (Figures 4a,b and 7a,b). Hence, the porphyrin chromophores of the D1–D2–cyt *b*559 complex can be classified into two spectroscopic groups. Group I chromophores have an absorption maximum at 672 nm. Group II chromophores have an absorption maximum at 679 nm in freshly prepared D1–D2–cyt *b*559. When the complex is incubated in TX-100, the chromophores that absorb at 679 nm are converted to the 669-nm form with first-order kinetics. Having the rate constant *k*, one can calculate the percentage of D1–D2–cyt *b*559 complexes that contain the 679 and the 669 nm absorbing chromophores ([D1D2-679] and [D1D2-669], respectively) at a time *t* after incubation.

To calculate the absorbance (in relative units) of the D1–D2–cyt *b*559 preparation at a particular wavelength λ, one needs to sum the percentage of the different chromophore groups multiplied by their relative absorbance at λ:

$$A_\lambda^{D1D2} = A_\lambda^{669}[\text{D1D2-669}] + A_\lambda^{679}[\text{D1D2-679}] + A_\lambda^{672} + A_\lambda^{tail} \quad (3)$$

where the upper indices on the right-hand side are the wavelengths for maximum absorption of the different components shown in Figure 3c. Using this equation, we fit the experimental absorbances of different D1–D2–cyt *b*559 preparations and found that preparations with absorbance maxima at 674, 672, or 670.5 nm contain 80%, 40%, or 15% of the 679-nm component, respectively. These numbers coincide well with the descending quantum yields for the photochemical reduction of the primary acceptor, as reflected in the transient absorption of 450 nm (Table I), and for the reduction of silicomolybdate reported by McTavish et al. (1989).

Assignment of the D1–D2–Cyt b559 Absorption Components to Specific Pigments. When trying to understand the correlation between the absorption spectra dn photochemical activity, one first needs to identify the chromophores of each spectroscopic group. As we have shown, the D1–D2–cyt *b*559 complex contains four molecules of Chl*a* and two molecules of Phe*a*. Since the dipole strength of the lowest energy transition (Q_y) in free Chl*a* is 1.6–2 times that in free Phe*a* (Vernon, 1960), each Chl*a* should contribute ≈20% and each Phe*a* ≈10% of the long-wavelength band of the D1–D2–cyt *b*559 complex. Group II chromophores are related with the 679-nm absorption and contribute 35–40% of the Q_y transition as deduced from the absorption bleaching due to continuous illumination (Figure 3b) and the Gaussian deconvolution of the Q_y^{0-0} transition (Figure 3c). The line shape of these chormophores' absorption in the near-UV (Figure 3b) is typical of Chl*a* molecules. Note that if a Phe*a* molecule would contribute to the UV bleaching, it should have a maximum at 410–416 nm (where the Phe*a* has a maximum optical absorption) as long as the ratio between the bleached Phe*a* and Chl*a* is higher than 1:2. Hence, group II consists of two Chl*a* molecules. This leaves group I (maximum absorption at 672 nm) with the two (or three) other Chl*a* and the two Phe*a* molecules, including the Phe*a* acting as the primary electron acceptor.

In contrast to our interpretation, time-resolved optical spectroscopic studies of oxygen-evolving RC particles have assigned an absorption maximum at 679–680 nm to the primary electron donor of PSII (Van Gorkom et al., 1975) and at 680–682 nm to the primary electron acceptor (Ganago et al., 1982; Nanba & Satoh (1987). Takahashi et al. (1987) and Satoh (1989) have relied on these interpretations when analyzing the spectra of illuminated D1–D2–cyt *b*559 complexes. However if both assignments were correct, the 679-nm component that has been resolved in our study and by low-temperature optical absorption (Breton, 1989; Satoh, 1989; Van Dorssen et al., 1987) would be due to one molecule of Phe*a* [suggested by Ganago et al. (1982) to be the primary acceptor] and either one or two molecules of Chl*a* [depending on whether the primary donor (P-680) is a Chl*a* monomer or dimer] (Satoh, 1989). This interpretation means that bleaching of group II chromophores by a destructive illumination should result in a difference spectrum with maxima at 679, 545, 515, and 416 nm, as previously mentioned.

One way to account for the absorption decrease at 682 nm upon the reduction of a Phe*a* molecule is to assume an electrochromic shift of the 679-nm transition to a shorter wavelength (Ganago et al., 1982) that is accompanied by a small line broadening. In that case the reduction of a single Phe should result in a bleaching at 682 nm and a concomitant small absorption increase at a shorter wavelength as observed [i.e., Nanba and Satoh (1987)]. The dashed–dotted line in Figure 10 illustrates the predicted absorption difference due to the reduction of one Phe and the electrochromic shift (by 3 nm) of the 679-nm transition. It consists of an absorption decrease at 679 nm due to the subtraction of the group II absorption, an absorption decrease at 672 nm due to the Phe bleaching (dotted line), and an absorption increase at 676 nm due to the

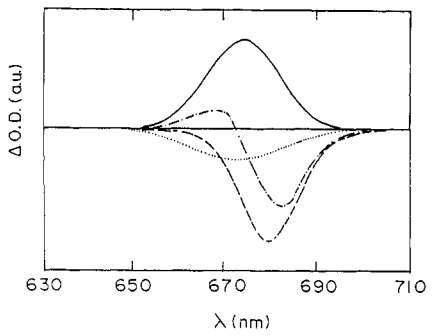

FIGURE 10: Simulation of the spectral change in the lowest energy absorption signal due to photochemical reduction of one Phe in the D1-D2-cyt *b*559. (···) The absorption decrease due to bleaching of one Phe equals one-sixth of the 672-nm Gaussian in Figure 3c. (– –) Absorption decrease due to the electrochromic shift of the 679-nm Gaussian (Figure 3c) from 679 nm. (—) Absorption increase due to the shift of the 679-nm Gaussian to 676 nm. (–·–) The sum of the three components showing an absorption decrease at 682 nm and absorption increase at ~670 nm.

addition of group II absorption. The sum of the solid and dashed lines should be polarized along the Q_y transitions of the two Chls in group II, and the dotted line shyould be polarized along the Q_y transition of the photoactive Phe. These predictions fit nicely the linear dichroism (LD) spectra of the D1-D2-cyt *b*559 complex recently published by Breton (1989), although Breton suggests that the Phe absorbs at ~678 nm.

Interpretation of the Optical Absorption, CD Spectra, and Fluorescence of the D1-D2-Cyt b559 Complex. The individual Chl*a* and Phe*a* molecules have four major electronic transitions termed Q_y, Q_x, B_x, and B_y in order of increasing energy. Each transition is optically active, but the rotational strengths are small. The Q_y transitions occur at 660–666 nm (depending on the coordination of the central Mg), and their bandwidth at half-maximum intensity is 390 cm^{-1} (in ether) to 530 cm^{-1} (in formamide–water/TX-100)(Scherz and Rosenbach-Belkin, unpublished data).

A major (narrow) Gaussian (350–420 cm^{-1}) and a minor (broad) Gaussian (550–680 cm^{-1}) can fit well the lowest energy transition (Q_y^{0-0} in different solvents (Cotton et al., 1974; Katz et al., 1978; Uehara et al., 1988). The narrow Gaussian contributes 90% or more of the dipole strength transition. Similar Gaussian deconvolution can be carried out on Chl aggregates in vitro (Katz et al., 1978; Uehara et al., 1988) and in vivo (French, 1972; Ikegami et al., 1988), but the number of components depends upon the aggregation number and the geometry of the aggregated molecules.

The spectroscopic properties of the Phe*a* and Chl*a* molecules in the D1-D2-cyt *b*559 complex are markedly different from their properties as in vitro monomers. Two Chls (group II) have their lowest energy transition at 679 nm. Since the full spectrum of these Chls is light dependent under nonreducing conditions (Figure 3b), it is reasonable to assign the light-dependent part of the CD signal (under the same nonreducing conditions) (Figure 5d, dashed–dotted line) to the same Chls. The other two Chl*a* and two Phe*a* molecules in the photochemically active D1-D2-cyt *b*559 complex probably absorb at 672–673 nm. The full spectrum of these pigments is light independent (under nonreducing conditions) (Figure 3a, dashed line), as is their CD spectrum (Figure 5c, dashed line). Apparently, the contributions of the Chl pair and the other chromophores are independent of each other to a first approximation.

We have considered (A) specific interactions among the pigments and the surrounding proteins and (B) interactions of the chromophores with each other, as two possible sources of the differences between the spectral properties of the D1-D2-cyt *b*559 complex and those of an equivalent mixture of Chl*a* and Phe*a* in vitro.

(A) Protein-induced chirality and bathochromic shift of the Q_y transition have been suggested to explain the spectral properties of P-860 and P-960, the primary electron donors of purple bacteria (Eccles et al., 1983). Studies by Boxer and Wright (1979), Wright and Boxer (1981), Davis et al. (1982), Kuki and Boxer (1983), and Woody (1984) using chlorophyllide-substituted myoglobins showed a small red shift (4–6 mm) of the lowest energy absorption and a protein-induced inversion of the chlorophyllide CD signal that was accompanied by a 3-fold increase of the rotational strength. Extrapolation from these experiments led Maggiora et al. (1985) and Wasielewski et al. (1989) to suggest that the bathochromic shift of the Chls' lowest energy absorption (when compared to that of in vitro monomers) primarily results from interactions with the protein. However, the Chls and the Phes in the D1-D2-cyt *b*559 complex evidently do not meet the criteria for such effects of the protein. First, on the basis of the homology with the proteins of the purple bacteria, the D1-D2-cyt *b*559 apoproteins do not contain charged amino acid residues near the Chl*a* pair (Michel & Deisenhofer, 1988). Second, during the incubation with TX-100 the native structure of the D1-D2 apoproteins and their chirality are probably conserved, as found for the proteins of the bacterial RCs (Nozawa et al., 1986). Therefore if the Cd of the complex is induced by the protein chirality, it should be preserved during incubation as long as the pigments are attached to their apoproteins. But as we have shown, the CD signal decays upon incubation although recent gel electrophoresis under nondissociating conditions has indicated that the Chl and the Phe molecules do not dissociate from the proteins (Braun and Scherz, unpublished data). Third, the CD signal at 669 nm is not accompanied by an electronically allowed transition. The small Gaussian that has been resolved at this wavelength in the initial absorption spectrum (Figure 3c) is probably due to an early degradation of some D1-D2-cyt *b*559 complexes and is not an intrinsic component of the intact complex. This component increases during incubation with TX-100 while the CD signal decreases.

(B) The second explanation is that some of the porphyrins interact with each other and these interactions affect their spectra. Sauer and co-workers noted already 2 decades ago that a bathochromic shift of the Q_y transition and strong CD signals can be induced by exciton coupling in Chl dimers in CCl_4 (Dratz et al., 1967; Houssier et al., 1970). Katz and collaborators have interpreted the absorption shift in terms of donor–acceptor interactions among the aggregated Chls [for a leading review, see Katz et al. (1978)]. Other groups concentrated on the spectroscopic properties of Chl aggregates in pure and mixed aqueous solutions (Katz et al., 1978; Boxer, 1983; Boddi & Lang, 1981; Gottstein & Scheer, 1983; Watanabe, 1985; Schmidt et al., 1989; Scherz & Rosenbach-Belkin, 1989; Scherz et al., 1988a,b, 1989a,b; Gottstein and Scheer, unpublished data). Similar observations were reported for bacteriochlorophylls (Bchl) and bacteriopheophytin (Bphe) (Gottstein & Scheer, 1983; Scherz & Parson, 1984a; Scherz et al., 1985, 1989a,b; Scherz & Rosenbach-Belkin, 1989; Rosenbach-Belkin & Scherz, 1989).

All these cases were characterized by (a) splitting of the Q_y transition, (b) shifting of the gravity center of the two new transitions to a longer wavelength relative to the Q_y transition of the individual chromophores, and (c) induction of a non-

Table II: Experimental and Calculated Spectral Properties of Chl*a*, Phe*a*, and Their in Vivo Pairs

	Q_y			Q_z			$B_{x,y}$[e]	
	λ_{max} (nm) [$\Delta\nu$ (cm^{-1})]	dipole strength (D^2)[d]	rotat strength (D μ_B)[e,f]	λ_{max} (nm)	dipole strength (D^2)[d]	rotat strength (D μ_B)[e,f]	λ_{max} (nm)	dipole strength (D^2)[d]	rotat strength (D μ_B)[e,f]
Chl^P[a]	669 (520)	21.0	−0.14	575	0.016		431	144	+0.018
Chl^a[a]	672 (520)	21.0	−0.14	575	0.016		431	144	+0.018
Phe[a]	672 (520)	16.0	−0.08	535	0.030	+0.052	416	150	+0.036
							439	145	+6.41
	680 (300)	47.0	+1.00	575	0.003	−0.003	435	9	−8.30
Chl^P–Chl^P[b,f,g]	668 (300)	2.0	−0.60	574.9	0.033	+0.002	426	91	+7.60
							419	12	−6.00
							431	44	+1.50
	672.5 (520)	49.0	−2.62	575	0.015	+0.001	429	100	−0.07
Chl^A–Phe[c,f,g]	671.5 (520)	18.0	+2.57	530	0.107	−0.000	416	44	+0.50
							409	99	−1.91

[a] Chl^P and Chl^A stand for the individual Chl in P-680 and the accessory Chl, respectively. [b] In the Chl*a* dimer, one Chl*a* molecule is centered at the origin, and the other one is at $-2x$, $-8y$, $+6z$, where y and x are along the N_1–N_3 and N_2–N_4 directions of the first Chl*a* molecule. z is along the normal to the first molecule plan. The angles between the transition dipoles are as follows: $Q_y^2Q_y^1$, 150°; $Q_x^2Q_y^1$, 117°; $Q_y^2Q_x^1$, 112°; $Q_x^2Q_x^1$, 28°. The angles between the transition dipoles are as follows: $Q_y^2Q_y^1$, 150°; $Q_x^2Q_y^1$, 117°; $Q_y^2Q_x^1$, 112°; $Q_x^2Q_x^1$, 28°. The angles between the normal to the Chl1 and the Chl2 transition dipoles are as follows: $Q_y^2Z^1$, 70°; $Q_x^2Z^1$, 100°. [c] In the Chl*a*–Phe*a* heterodimer the Chl*a* is centered at the origin, and the Phe*a* is at $-2x$, $-8.5y$, $+8.5z$. The angles between the transition dipoles are as follows: $Q_y^2Q_y^1$, 80°; $Q_x^2Q_y^1$, 10°; $Q_y^2Q_x^1$, 158°; $Q_x^2Q_x^1$, 79°. The angles between the normal to the Chl*a* and the Phe*a* transition dipoles are as follows: $Q_y^2Z^1$, 70°; $Q_x^2Z^1$, 90°. [d] We only considered the dipolar strength of the 0–0 transition because the exciton splitting is comparable to the bandwidth of the 0–0 transition. The dipole strength given in debyes squared (D^2) equals $(9.18 \times 10^{-3})\int \epsilon(\nu)\nu^{-1}\, d\nu$, where ϵ is the extinction coefficient (in mol^{-1} cm^{-1}) and ν is the wavenumber (cm^{-1}) for maximum absorption. [e] The position of the B_x and B_y transitions relies upon the MCD report of Houssier and Sauer (1970). The total dipolar strength may be overestimated due to a contribution from higher energy transitions (Weiss, 1972). [f] The experimental rotational strength R is given in units of debye Bohr magneton, where $R = 0.248\int \Delta\epsilon(\nu)\nu^{-1}\, d\nu$. [g] The theoretical calculation followed Scherz and Parson (1984b). However, we have postulated a nonexcitonic shift from 669 to 673.5 nm due to nonexcitonic interactions among the paired molecules [see text and Rosenbach-Belkin and Scherz (1989) for further discussion].

conservative CD doublet. As the relative intensity of the two new transitions, their bathochromic shift, and their rotational strength depend upon the geometry of the dimer (Houssier & Sauer, 1970; Boxer, 1983; Scherz & Parson, 1984a; Warshel & Parson, 1987; LaLonde et al., 1989), the spectral resemblance between the in vitro Chl dimers and the in vivo Chl culsters suggests a common structural motif (Scherz & Rosenbach-Belkin, 1989). By simulating the dimer absorption and CD, it is therefore possible to roughly determine the dimer geometry (Tinoco, 1962; Houssier & Sauer, 1970; Scherz & Parson, 1984b; Parson et al., 1985; Warshel & Parson, 1987; LaLonde et al., 1989). When the separation between the paired molecules is larger than their sizes, the point dipole approximation can be used (Tinoco, 1962). For smaller separation, the point monopole approximation (Tinoco, 1962; Murrell & Tanaka, 1964; Parson & Warshel, 1987; LaLonde et al., 1989) should be used. There are several advantages to the point dipole approximation: (a) it does not rely upon the accuracy of the calculated molecular orbitals, and (b) it provides the transitions' energy, oscillator strength, and rotational strength in a straightforward manner. Obviously, when the geometry of the interacting pigments is unknown, another criterion for selecting the appropriate approximation is needed, a simple one being the difference between the interaction energies calculated by the two approaches. If the energies are roughly equal, the point dipole approach can be chosen (Pearlstein, 1982).

Following these lines, we calculated the geometry of Chl*a* dimer having the Q_y transitions of the individual molecules at 673 nm (the gravity center for the light-dependent CD signal of the D1–D2–cyt *b*559 complex under nonreducing conditions) and the Q_y transition of the excitonically coupled pair at 679 nm. We assumed the following: (a) This Q_y transition of each pigment consists of two Gaussians, one of which (Q_y^{0-0}) carries over 90% of the dipolar strength, as observed by Cotton et al. (1974) for the Q_y^{0-0} of Chl*a* monomers in most protic solvents. (b) Having most of the Q_y dipole strength, the narrow Gaussians give rise to the 679-nm absorption and the 679- and 669-nm couplets in the light-dependent CD signal due to the two group II Chls (Figure 5e). (c) As the energy difference between the CD couplets at 679 and 669 nm (220 cm^{-1}) is smaller than the energy difference between the Q_y^{0-0} and Q_y^{0-1} transitions of the individual Chl*a* molecules (≈300 cm^{-1}), one should consider separately the coupling among the different vibronic states (Simpson & Peterson, 1957). Since the intensity of the Q_y^{0-0} transition is about 10 times the Q_y^{0-1} intensity and the exciton splitting is proportional to the square of these intensities, one expects the red-most Gaussian in the D1–D2–cyt *b*559 complex to be contributed by the lower energy excitonic transition of Q_y^{0-0}.

A geometry that provides the spectral properties of the Chl*a* pair (Table II), with the point dipole approximation (Scherz & Parson, 1984b), resembles the special pair geometry in the bacterial RC (see footnote *b* in Table II). However, the center-to-center separation among the Chl*a* molecules is larger by about 3 Å, generally along the Q_y transition dipole but also perpendicular to the molecular planes. This simulation does not provide any information about the orientation of the dimer transitions with respect to the membrane plane. However, judging from the electrochromic shift of the 679-nm transition (Figure 9, sum of dashed and solid lines) in comparison with the light-dependent linear dichroism (Breton, 1989), and Q_y transition should be roughly parallel to the membrane plane.

To confirm the validity of the point dipole approach, the dipolar interaction within the proposed geometry was calculated (J. R. E. Fisher and Scherz, unpublished data) with the Q_y transition monopoles [given by Weiss (1972)] in the split-mode fashion (Philipson & Sauer, 1972; Pearlstein, 1988; Scherz & Rosenbach-Belkin, 1989). The difference between the interaction energy calculated by the point monopole and point dipole approximation was less than 20%.

In the calculated geometry the separation between the two π centers does not allow for appreciable overlap of the molecular orbitals, and therefore, the contribution of charge transfer states should be minimal. If the simulated geometry represents the geometry of P-680, it provides an explanation

for the failure to observe a Stark effect in the D1–D2–cyt *b*559 complex (Satoh, 1989; Losche et al., 1989) and for the triplet–singlet spectrum that has been reported by den Blanken et al., (1983), since the large separation assures the localization of a triplet excited state on one of the Chls. On the other hand, the exciton coupling is strong enough to make the Chl pair an energy trap in the PSII RC, as required for the primary electron donor.

We have suggested that group I porphyrins (two Chl*a* and two Phe*a* molecules) contribute the 672 nm absorption Gaussian and the light-independent (in the absence of reducing agents) CD signals at 673 (+) and 671 (−) nm. There are probably several configurations in which excitonic interactions among two Chls and two Phes could result in these spectral properties. One possibility is that the pigments make two heterodimers where the individual molecules are roughly perpendicular to each other (Table II) and their centers separated by ~12 Å. The CD signals and the optical absorption calculated for this configuration with the extended exciton theory in the point dipole approximation (Scherz & Parson, 1984b) are shown in Table II. Note that the pigment organization in the proposed configuration resembles the configuration suggested by Breton (1989) from linear dichroism measurements, and the organization of the analogous pigments in the bacterial RC (Deisenhofer et al., 1985).

Rationalization of the TX-100-Induced Changes in Spectra and Photochemical Activity. According to our data, but contrary to the conclusion of Tetenkin et al. (1989), the detergent-induced changes in spectra and photochemical activity of the D1–D2–cyt *b*559 complex are both related to a modification of the two Chl*a* molecules that initially absorb at 679 nm. The rate of modification of the 679 nm absorbing Chls is inversely proportional to the concentration of the D1–D2–cyt *b*559 complex and directly proportional to the concentration of TX-100 (data not shown), suggesting that the process involves dissociation of D1–D2–cyt *b*559 aggregates into single D1–D2–cyt *b*559 units. The configuration of the polypeptides and their attached Chls in these units evidently is very labile. Assuming that each of the special pair Chls is attached to a different polypeptide, the polypeptide conformation in the dissociated units could alter the exciton coupling, so that the pigments regain their individual absorption at 669 nm. Hence, the lowest energy excited state of the D1–D2–cyt *b*559 complex is shifted into group I Chls and Phes, which have an absorption maximum at around 672 nm. These pigments cannot provide a channel for nonradiative decay and therefore fluoresce (at 679 nm) with a quantum yield similar to that of free Chls and Phes.

Concluding Remarks. The pigment content in D1–D2–cyt *b*559 complexes have been isolated in TX-100-containing solutions resembles the pigment content in the bacterial RCs. The dimeric nature of the primary donor and the configuration of the primary acceptor and the accessory pigments appear to be similar. In both RCs, the primary donors absorb at longer wavelengths than the primary acceptors. However, the separation between the Chls in P-680 evidently is substantially larger than that in the bacterial RCs. Electron spin resonance studies of the PSII triplet state (Rutherford et al., 1986) and linear dichroism measurements (Breton, 1989) indicate that at least one of the P-680 Chls is almost parallel to the membrane plane, in contrast to the Bchls in P-960 or P-860.

Scherz et al. (1985, 1989a,b) and Scherz and Rosenbach-Belkin (1989) have shown that Chls and Bchls tend to associate into particular $\pi-\pi$ dimers. The self-dimerization involves a large free energy change and may add to the protein stability (Scherz & Rosenbach-Belkin, 1989, Scherz et al., 1989b). These dimers are characterized by a much larger bathochromic shift than observed for the Q_y transition of P-680, indicating that the protein environment of the special pair in the D1–D2–cyt *b*559 complex does not allow such self-assembly. In addition to pointing at a significant difference from the protein surrounding of the bacterial special pair, this may account in part for the low stability of P-680 relative to the bacterial primary donors and the high turnover of the D1 apoprotein in vivo (Matoo et al., 1984).

Added in Proof

Kobayashi et al. (1985) have recently reported that the D1–D2–cyt *b*559 complex isolated in digitonin-containing solutions holds six Chls to each two Phes. A comparison of their pigment–acetone extract with the one we obtained from our D1–D2–cyt *b*559 preparation (isolated in the TX-100-containing solutions) indicates indeed a higher Chl content. Obviously, the TX-100 treatment released two Chls, which probably act as antenna pigments. It also seems to release one of the carotenoides, the level of which is higher in their preparation.

Acknowledgments

We are grateful to Prof. M. Edelman and Mr. H. Kless from the Department of Plant Genetics, Weizmann Institute of Science, for thorough discussions and critical comments. We are also grateful to Dr. J. B. Marder and Prof. J. Barber from the AFRC Photosynthesis Research Group of the Imperial College for guiding us in the first preparation of PSII RCs.

Registry No. Chl*a*, 479-61-8; Phe*a*, 603-17-8; P680, 53808-91-6; TX-100, 9002-93-1; cytochrome *b*-559, 9044-61-5.

References

Allen, J. P., Feher, G., Yeates, T. O., Komiya, H., & Rees, D. C. (1987) *Proc. Natl. Acad. Sci. U.S.A. 84*, 6162–6166.

Barber, J., Chapman, D. J., & Telfer, A. (1987a) *FEBS Lett. 220*, 67–73.

Barber, J., Gounaris, K., & Chapman, D. J. (1987b) in *Cytochrome Systems* (Papa, S., Chance, B., & Ernster, L., Eds.) pp 657–666, Plenum Press, New York.

Ben-Amotz, A., Shaish, A., & Avron, M. (1989) *Plant Physiol.* (in press).

Boddi, K. K., & Lang, F. (1981) *Photobiochem. Photobiophys. 2*, 321–328.

Boxer, S. G. (1983) *Biochim. Biophys. Acta 726*, 265–292.

Boxer, S. G., & Wright, K. A. (1979) *J. Am. Chem. Soc. 101*, 6791–6794.

Braun, P., Greenberg, B., & Scherz, A. (1988) in *Abstracts of The Second International Congress of Plant Molecular Biology* (Edelman, M., Ed.) Jerusalem, 1988, Abstract 392, Weizmann Institute of Science.

Breton, J. (1989) in *Perspectives in Photosynthesis* (Jortner, J., & Pullman, B., Eds.) Jerusalem Symposia on Quantum Chemistry and Biochemistry 22, pp 23–38, Kluwer Academic Publishers, Dordrecht, The Netherlands.

Butler, W. L., & Hopkins, D. W. (1970) *Photochem. Photobiol. 12*, 439–450.

Chang, H., Tiede, D., Tang, J., Smith, U., Norris, J. R., & Schiffer, M. (1986) *FEBS Lett. 205*, 82.

Chapman, D. J., Gounaris, K., & Barber, J. (1988) *Biochim. Biophys. Acta 933*, 423–431.

Connolly, J. S., Samuel, E. B., & Janzen, A. E. (1982) *Photochem. Photobiol. 36*, 565–574.

Cotton, T. M., Trifunac, A. D., Ballschmitter, K., & Katz, J. J. (1974) *Biochim. Biophys. Acta 368*, 181–198.

Deisenhofer, J., Epp, O., Miki, K., Huber, R., & Michel, H. (1985) *Nature 318*, 618–624.

Dekker, J. P., Bowlby, N. R., & Yocum, C. F. (1989) *FEBS Lett. 254*, 150–154.

Den Blanken, H. J., & Hoff, A. J. (1982) *Biochim. Biophys. Acta 681*, 365–374.

Den Blanken, H. J., Hoff, A. J., Jongenelis, A. P. J. M., & Diner, B. (1983) *FEBS Lett. 157*, 21–27.

Dratz, E. A., Schultz, A. J., & Sauer, K. (1967) in *Energy Conversion By the Photosynthetic Apparatus* (Olson, J. J., Ed.) *Brookhaven Symp. Biol. 19*, 303–318.

Eccles, J., & Honig, B. (1983) *Proc. Natl. Acad. Sci. U.S.A. 80*, 4959–4962.

Feher, G., Isaacson, R. A., & Anderson, L. C. (1975) *Ann. N.Y. Acad. Sci. 244*, 239–254.

French, C. S., Brown, J. S., & Lawrence, M. C. (1972) *Plant Physiol. 49*, 421–429.

Ganago, I. B., Klimov, V. V., Ganago, A. O., Shuvalov, V. A., & Erokhin, Y. E. (1982) *FEBS Lett. 140*, 127–130.

Gottstein, J., & Scheer, H. (1983) *Proc. Natl. Acad. Sci. U.S.A. 30*, 2231–2234.

Hearst, J. E., & Sauer, K. (1984) in *Advances in Photosynthetic Research* (Sybesma, C., Ed.) Vol. III, pp 355–359, Martinus Nijhoff/Dr. W. Junk, The Hague, The Netherlands.

Hemenger, R. P. (1977) *J. Chem. Phys. 67*, 262–264.

Houssier, C., & Sauer, K. (1970) *J. Am. Chem. Soc. 92*, 779–791.

Ikegami, I., & Shigura, I. (1988) *Biochim. Biophys. Acta 934*, 39–46.

Katz, J. J., Shipman, L. L., Cotton, T. M., & Janson, T. R. C. (1978) in *The Porphyrins* (Dolphin, D., Ed.) pp 401–456, McGraw-Hill, New York.

Kobayashi, M., Maedar, H., Watenabe, T., Nakane, H., & Satoh, K. (1990) *FEBS Lett. 260*, 138–140.

Kuki, A., & Boxer, S. G. (1983) *Biochemistry 22*, 2923–2933.

Laemmli, U. K. (1970) *Nature 227*, 680–685.

LaLonde, D. E., Petke, J. D., & Maggiora, G. M. (1989) *J. Phys. Chem. 93*, 608–614.

Lichtenthaler, H. K. (1987) *Methods Enzymol. 148*, pp 351–382.

Losche, K., Satoh, K., Feher, G., & Okamura, M. Y. (1988) *Biophys. J. 53*, 270a.

Maggiora, L. L., Petka, J. D., Gopal, D., Iuramoto, R. T., & Maggiora, G. M. (1985) *Photochem. Photobiol. 42*, 69–75.

Marder, J. B., Matoo, A. K., & Edelman, M. (1986) *Methods Enzymol. 118*, 384–396.

Marder, J. B., Chapman, D. J., Telfer, A., Nixon, P. J., & Barber, J. (1987) *Plant Mol. Biol. 9*, 325–333.

Matoo, A. K., Hoffman, F., Marder, J. B., & Edelman, M. (1984) *Proc. Natl. Acad. Sci. U.S.A. 81*, 1380–1384.

McTavish, H., Picorel, R., & Seibert, M. (1989) *Plant Physiol. 89*, 452–456.

Michel, H., & Deisenhofer, J. (1988) *Biochemistry 27*, 1–7.

Murrell, J. N., & Tanaka, J. (1964) *Mol. Phys. 7*, 363–380.

Nanba, O., & Satoh, K. (1987) *Proc. Natl. Acad. Sci. U.S.A. 84*, 109–112.

Newell, W. R., van Amerongen, H., van Grondelle, R., Aalberts, J. W. Drake, A. F., Udvarhelyi, P., & Barber, J. (1988) *FEBS Lett. 228*, 162–166.

Norris, J. R., Uphaus, R. A., Crespi, H. L., & Katz, J. J. (1971) *Proc. Natl. Acad. Sci. U.S.A. 68*, 625–629.

Norris, J. R., Scheer, H., & Katz, J. J. (1975) *Ann. N.Y. Acad. Sci. 244*, 261–280.

Nozawa, T., Ohta, M., Hatano, M., Hayashi, H., & Shimada, K. (1986) *Biochim. Biophys. Acta 850*, 343–351.

Okamura, M. Y., Feher, G., & Nelson, N. (1982) in *Photosynthesis: Energy Conversion in Plants & Bacteria* (Govindjee, Ed.) pp 195–272, Academic Press, Orlando, FL.

Omata, T., & Murata, N. (1980) *Photochem. Photobiol. 31*, 183–185.

Parson, W. W., & Warshel, A. (1987) *J. Am. Chem. Soc. 109*, 6154–6163.

Parson, W. W., Holten, D., Kirmaier, A., Scherz, A., & Woodbury, N. (1984) in *Advances in Photosynthesis Research, Proceedings Research, Proceedings of the VI International Congress on Photosynthesis* (Sybesma, C., Ed.) Vol. 1, pp 187–193, Martinus Nijhoff, Dordrecht, The Netherlands.

Parson, W. W., Scherz, A., & Warshel, A. (1985) in *Antennas & Reaction Centre of Photosynthetic Bacteria* (Michel-Beyerle, M., Ed.) *Springer Ser. Chem. Phys. 42*, 122–130.

Pearlstein, R. M. (1982) In *Energy Conversion by Plants & Bacteria* (Govindjee, Ed.) Vol. 1, pp 293–330, Academic Press, Orland, FL.

Pearlstein, R. (1988) in *The Photosynthetic Bacterial Reaction Center, Structure & Dynamics* (Breton, J., & Vermeglio, A., Eds.) *NATO ASI Ser., Ser. A 149*, 331–339.

Peter, F. P., & Thornber, P. (1988) in *Photosynthetic Light Harvesting Systems* (Scheer, H., & Schneider, S., Eds.) pp 175–186, Walter de Gruyter, Berlin.

Peter, F., & Thornber, P. (1989) in *Amino Acids, Proteins & Nucleic Acids* (Rogers, L. J., Ed.) *Methods Plant Biochem.* (in press).

Philipson, K. D., & Sauer, K. (1972) *Biochemistry 11*, 1880–1885.

Posner, H. B. (1967) in *Methods in Developmental Biology* (Witt, F. A., & Wessels, S. N. K., Eds.) pp 301–317, Crowell, New York.

Rosenbach-Belkin, V., & Scherz, A. (1989) *J. Am. Chem. Soc.* (in press).

Rutherford, A. W. (1985) *Biochim. Biophys. Acta 807*, 189–201.

Satoh, K. (1989) in *Photochemical Energy Conversion, Proceedings of the VII International Conference on Photochemical Conversion & Storage of Solar Energy* (Norris, J. R., & Meisel, D., Eds.) pp 238–250, Elsevier, Amsterdam.

Scherz, A., & Parson, W. W. (1984a) *Biochim. Biophys. Acta 766*, 653–665.

Scherz, A., & Parson, W. W. (1984b) *Biochim. Biophys. Acta 766*, 665–678.

Scherz, A., & Parson, W. W. (1986) *Photosyn. Res. 9*, 19–30.

Scherz, A., & Rosenbach-Belkin, V. (1989) *Proc. Natl. Acad. Sci. U.S.A. 86*, 1505–1509.

Scherz, A., Rosenbach-Belkin, V., & Malkin, S. (1985) in *Antennas & Reaction Center of Photosynthetic Bacteria* (Michel-Beyerle, M., Ed.) *Springer Ser. Chem. Phys. 42*, 314–323.

Scherz, A., Braun, P., Greenberg, B., Marder, J., & Barber, J. (1988a) in *Abstracts of the Second International Congress of Plant Molecular Biology* (Edelman, M., Ed.) Jerusalem, 1988, Abstract 391, Weizmann Institute of Science.

Scherz, A., Rosenbach-Belkin, V., & Fisher, J. R. E. (1989) in *Perspectives in Photosynthesis* (Jortner, J., & Pullman,

B., Eds.) Jerusalem Symposia on Quantum Chemistry and Biochemistry 22, pp 371–381, Kluwer Press, Dordrecht, The Netherlands.
Scherz, A., Rosenbach-Belkin, V., & Fisher, J. R. E. (1990) *Proc. Natl. Acad. Sci. U.S.A. 87*, 5430–5434.
Schmidt, A., Gottstein, J., Scheer, M., & Scherz, A. (1990) *Z. Naturforsch.* (in press).
Seibert, M., Picorel, R., Rubin, A. B., & Connolly, J. S. (1988) *Plant Physiol. 87*, 303–306.
Shuvalov, V. A., & Asadov, A. A. (1979) *Biochim. Biophys. Acta 545*, 296–308.
Simpson, W. T., & Peterson, D. L. (1957) *J. Chem. Phys. 26*, 588–589.
Straley, S. C., Parson, W. W., Mauezerall, D., & Clayton, R. K. (1973) *Biochim. Biophys. Acta 405*, 597–609.
Takahashi, Y., Hansson, O., Mathis, P., & Satoh, K. (1987) *Biochim. Biophys. Acta 893*, 49–59.
Tetenkin, V. L., Gulgaeve, B. A., Seibert, M., & Rubin, A. B. (1989) *FEBS Lett. 250*, 459–463.
Thornber, P., Peter, G. F., Nechushtai, R., Chitnis, P. R., Hunter, F. A., & Tobbin, E. M. (1986) in *Regulations of Chlorophyll-Protein Complexes & Their Apoproteins* (Akogunoglou, G., & Senger, H., Eds.) pp 249–258, A. R. Liss, New York.
Thornber, P., Peter, G. F., & Nechushtai, R. (1987) *Physiol. Plant 71*, 231–240.
Tinoco, I., Jr. (1962) *Adv. Chem. Phys. 4*, 113–157.
Trebst, A., & Depka, B. (1985) in *Antenna & Reaction Centres of Photosynthetic Bacteria—Structure, Interactions & Dynamics* (Michel-Byerelye, M. E., Ed.) *Springer Ser. Chem. Phy. 42*, 215–223.
Uehara, K., Mimuro, M., Fujita, Y., & Makota, T. (1988) *Photochem. Photobiol. 48*, 725–732.
Van Dorssen, R. J., Breton, J., Plijter, J. J., Satoh, K., van Gorkom, H. J., & Amesz, J. (1987) *Biochim. Biophys. Acta 893*, 267–274.
Van Gorkom, H. J., Pulles, P. J., & Wessels, J. S. C. (1975) *Biochim. Biophys. Acta 408*, 331–339.
Vermeglio, A., & Clayton, R. K. (1976) *Biochim. Biophys. Acta 449*, 500–515.
Vernon, L. P. (1960) *Anal. Chem. 32*, 1144–1150.
Warshel, A., Creighton, S., & Parson, W. W. (1988) *J. Phys. Chem. 92*, 2696–2701.
Wasielewski, M., Johnson, D. G., Seibert, M., & Govindjee (1989a) *Proc. Natl. Acad. Sci. U.S.A. 86*, 524–528.
Wasielewski, M., Johnson, D. G., Govindjee, Preston, C., & Seibert, M. (1989b) *Photosynth. Res. 22*, 89–99.
Watanabe, T., Kobayashi, M., Hongu, A., Nakazato, M., Hiyama, T., & Murata, N. (1985) *FEBS Lett. 191*, 252–256.
Weiss, C. (1972) *J. Mol. Spectrosc. 41*, 37–80.
Williams, J. C., Steiner, L. A., Feher, G., & Simon, M. J. (1984) *Proc. Natl. Acad. Sci. U.S.A. 81*, 7303–7307.
Woody, R. W. (1984) in *Optical Properties & Structure of Tetrapyrroles* (Blauer, G., & Sund, H., Eds.) pp 340–354, Reidel, Dordrecht, The Netherlands.
Wright, K. A., & Boxer, S. G. (1981) *Biochemistry 20*, 7546–7556.

Monoclonal Antibody Modification of the ATPase Activity of *Escherichia coli* F_1 ATPase†

Robert Aggeler, Janet Mendel-Hartvig, and Roderick A. Capaldi*
Institute of Molecular Biology, University of Oregon, Eugene, Oregon 97403
Received June 21, 1990; Revised Manuscript Received August 1, 1990

ABSTRACT: Monoclonal antibodies (mAbs) have been made against each of the five subunits of ECF_1 (α, β, γ, δ, and ϵ), and these have been used in topology studies and for examination of the role of individual subunits in the functioning of the enzyme. All of the mAbs obtained reacted with ECF_1, while several failed to react with ECF_1F_0, including three mAbs against the γ subunit (γII, γIII, and γIV), one mAb against δ, and two mAbs against ϵ (ϵI and ϵII). These topology data are consistent with the γ, δ, and ϵ subunits being located at the interface between the F_1 and F_0 parts of the complex. Two forms of ECF_1 were used to study the effects of mAbs on the ATPase activity of the enzyme: ECF_1 with the ϵ subunit tightly bound and acting to inhibit activity and ECF_1* in which the δ and ϵ subunits had been removed by organic solvent treatment. ECF_1* had an ATPase activity under standard conditions of 93 μmol of ATP hydrolyzed min^{-1} mg^{-1}, cf. an activity of 7.5 units mg^{-1} for our standard ECF_1 preparation and 64 units mg^{-1} for enzyme in which the ϵ subunit had been removed by trypsin treatment. The protease digestion of ECF_1* reduced activity to 64 units mg^{-1} in a complicated process involving an inhibition of activity by cleavage of the α subunit, activation by cleavage of γ, and inhibition with cleavage of the β subunit. mAbs to the γ subunit, γII and γIII, activated ECF_1 by 4.4- and 2.4-fold, respectively, by changing the affinity of the enzyme for the ϵ subunit, as evidenced by density gradient centrifugation experiments. The γ-subunit mAbs did not alter the ATPase activity of ECF_1*- or trypsin-treated enzyme. The α-subunit mAb (αI) activated ECF_1 by a factor of 2.5-fold and ECF_1F_0 by 1.3-fold, but inhibited the ATPase activity of ECF_1* by 30%.

Monoclonal antibodies are being used extensively to study structure–function relationships of the F_1 ATPases of bacteria, plants, and animals [e.g., see Moradi-Ameli and Godinot (1983, 1987), Dunn et al. (1985), and Hadikusumo et al. (1984)]. Included in these studies are examination of cross-reactivity of F_1 ATPases from different organisms [e.g., see

† Supported by NIH Grant HL24236.

0006-2960/90/0429-10387$02.50/0